Penetration of long rods into semi-infinite metallic targets over wide range of impact velocities

Penetration of long rods into semi-infinite metallic targets over wide range of impact velocities

M A Abdel-Kader[1], A M Riad[1,2]andA Z Ibrahim[1]
[1]Weapons and Amm.Dept., Mechanical Engineering Branch, Military Technical College, Kobri El-Kobba, Cairo, Egypt.
[2] Corresponding author, Email: ahmed.riad@mtc.edu.eg.

Abstract. In this paper, the analytical model that describes the penetration process of a long rod into a semi-infinite metallic target over wide range of impact velocities has been presented. In this model, the target strength factor $R_t$is not considered as a constant but it is a function of penetration velocity whereas, the rod strength factor Y_P is represented by Hugoniot Elastic Limit (HEL) of its material. The penetration process of the present model consists mainly of primary phase during which the rod front is subjected to erosion and secondary (after-flow) phase. The main equations of the used model are presented, arranged and compiled into a computer program. The program is capable of predicting the time histories of the parameters associated with the penetration process. Autodyn hydrocode package is used herein to simulate the penetration processes of long rods into targets examined by the present analytical model. The hydrocode is fed with the same data used in the model for rods and targets materials. Both the model predictions and the obtained numerical results of Auto dynhydro code, respectively, are compared with the corresponding experimental measurements of other investigators. Good agreement is generally obtained. In addition, representative samples of the model predictions and their corresponding simulation results of Autodyn hydro code are presented with relevant analyses and discussions. The obtained results prove the predictive capabilities of both the present model and Autodyn hydro code, respectively, where each of them could be used as a quick tool for determining the main parameters associated with the studied penetration process.

1. Introduction

Long rod penetrators with large aspect ratios (length to diameter) have been widely used with the modern kinetic energy projectiles. These penetrators have high specific impact energies and great penetration capabilities to the modern armors. Very dense materials are used for manufacturing these penetrators such as tungsten alloys and depleted uranium. The penetration of high speed long rods into metallic targets has been studied experimentally, analytically and numerically since long time ago.

The developed one-dimensional hydrodynamic theories of penetration by Alekseevski [1] and Tate [2] have been used as reference models for describing the penetration of high-speed long rods into semi-infinite metallic targets. Both models contained two strength factors for target and rod materials; they denoted byR_t and Y_p, respectively. Both factors were determined experimentally. Tate used the Hugoniot Elastic Limit (HEL) of the rod material for Y_p and a value of 3.5 x HEL of the target material for R_t. Their models are capable of predicting the penetration depth and the rod deceleration into target.

Jones et al. [3] modified Tate's model of Ref. [2] by incorporating the mushroom-type deformation at the impact end of the rod and the deceleration of rod rigid end. The predicted penetration depths using Tate's model were inconsistent with those predicted by Jones et al. model for the same material strength factors. They attributed this difference to the lack of mushroom at the rod front in Tate's model. Wilson et al. [4] conducted an experimental program to check the validity of Jones et al. predictions.They got a quite good agreement between their measurements and the predictions of Ref. [3].They also reported that it was possible to get better agreement when a velocity-dependent mushroom strain was considered in theirmodel.

He and Wen [5] analyzed the long rod penetration process into semi-infinite metallic targets based on energy balance. They considered that a part of kinetic energy of the long rod was remained in the ejected rod debris.Thisdebris may continue to penetrate the target causing secondary penetration especially when a dense rod impacted into a semi-infinite metallic target with high velocities. Their model predictions are in good agreement with test results of Refs. [6-7].

Several analytical models that describe the penetration of high speed long rod into semi-infinite and finite thickness metallic targets have been reviewed by Anderson [8]. Upon review, he deduced the followingmain points: i) for the target strength factor of the modified hydrodynamic models; however,it depended on material properties, Anderson et al. [9] showed that it also depended on the impact velocity, ii) the use of compressible cylindrical cavity expansion model gave a good agreement with experimental measurements at impact velocity below 2 km/s as noted by Chocron et al. [10] when values of material flow stresses consistent with the behavior of materials were used, iii) the analytical models based on conservation of momentum such as Walker-Anderson model [11] tended to be applicable to a wide range of materials and impact velocities, and iv) the area concerned with the penetration of multi-material layered targets by high speed long rod was neededfor further works.

Jiao and Chen [12] developed approximate solutions of the main equations representing Tate's model of Ref. [2]. In "theoretical solution", these equations were solved numerically to predict the parameters associated with the rod penetration into a semi-infinite target implicitly as function of time. They also derived another two sets of explicit approximate algebraic solutions based on the implicit solution deduced from the equations of Tate's model. In their first approximate solution, they considered that the tail and penetration velocities varied logarithmically with time while the other parameters were deduced from heir integrals. In their second approximate solution, they assumed that the tail and penetration velocities were constant and the other parameters varied linearly with time.They also derived a special case of first approximate solution named "first-order perturbation solution". The different solutions have been examined using the data for rods and targets of Refs. [13-14]. They found that the results of their first approximate solution were close to the theoretical predictions of Tate's model than other derived solutions. In addition, they strongly recommended this solution in engineering applications.

In the following, the analytical model of Ref. [15] that describes the penetration of a long rod into a semi-infinite metallic target is presented. The main phases and the considered assumptions in constructing the present model are introduced. In addition, the governing equations representing each penetration phase are presented. These equations are arranged and compiled into a computer program. The input data to the program are easily determined. Representative samples of the model predictions are presented and discussed. Autodyn 2D hydrocode is also used to assess the obtained analytical results.

2. Analytical model

In the present model, the projectile is idealized as a cylindrical rod with a hemispherical nose havinginitialshank length L_o and initial diameter D_o. The rod is assumed to strike the target normally with a high velocity. At such a velocity, Lan and Wen [15] reported that the ratio of shear stress to the pressure at rod-target interface can be neglected based on the numerical simulation results of Ref. [16]. Moreover, the behavior of the materials near the rod-target interface can be treated as a fluid similar to the one-dimensional model developed by Tate [2].Therefore, new response regions due to long rod

penetration intoa semi-infinite metallic target can be seen in figure 1 [15]. These regions along the penetration centerline are named by flow, plastic and elastic regions in the target; whereas the regions in the penetrating rod are named by flow and rigid tail regions. The points A, O and B on figure1 connect the penetration centerline with rigid flow interface in the rod, rod-target interface, flow plastic interface (FP) in the target, respectively. In the flow regions of rod and target, their materials are treated as non-viscous incompressible fluids. In addition, particle velocity and stress at the interface FP are continued in the normal directions. The penetration velocity is denoted by u;whereas thevelocity of rod rigid tail is denoted by v.

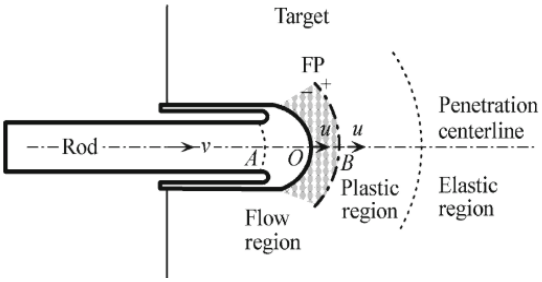

Figure 1. Response regions along the centerline at high impact velocity [15].

The present model identifies two different phases associated with the penetration of along rod into a semi-infinite metallic target; these are primary penetration phase and after-flow phase. At a high impact velocity, the primary penetration phase is dominated and the rod front is continuously erodedeven at low penetration velocity due to lateral confinement of the eroded rod. The velocity of rod rigid mass at which no flow region in the target V_C and the interface defeat velocity V_{ID} at which the penetration velocity u is equal to zero will be introduced, respectively.

For the primary penetration phase, a system of equations has been presented. The penetration time is taken as independent variable. This system is solved numerically to determine the time-histories of parameters associated with the penetration process. The current value of penetration velocity u is determined using its respective interface equation. In the following, the main assumptions considered during the analysis are introduced. In addition, the main equations and end conditions of the primary penetration phase are presented.

2.1.Main assumptions

- There exists a critical penetration velocity U_{Fo}. When the penetration velocity $u \geq U_{Fo}$, a flow region appears in the target; i.e. a thin layer appears in the target near the rod-target interface within which the material can be treated as “fluid” due to loss of its shear strength, otherwise there are only plastic and elastic regions.
- At the critical state ($u = U_{Fo}$), no particle passes through the interface FP, and U_{Fo} is equal to the velocity of the particle at position B; i.e. $\delta(u) = U_{Fo}$ where $\delta(u)$ is a function of u with defined field $[U_{Fo}, +\infty]$.
- When the penetration velocity u exceeds the critical penetration velocity U_{Fo}, the velocity of interface FP along the penetration direction is always equal to the penetration velocity u. This meansthat the width of the flow region remains constant during penetration so that the Bernoulli’s equation can be used which is applicable only in steady flow field.
- The cavity expansion model of Ref. [17] is applicable for predicting the displacement and velocity field of plastic and elastic regions.
- The function $\delta(u)$ decreases with increasing the penetration velocity u and tends to zero when u becomes infinity.
- As the rod decelerates, the pressure at the position O decreases with decreasing the penetration velocity u.

2.2. Governing equations

*2.2.1. Primary penetration phase.*When $u \geq U_{Fo}$, the flow field between points A and B can be treated as steady flow relative to position O. The particle velocity at position B is [u-δ(u)] relative to position O. When $u < U_{Fo}$, there is no flow region in the target. The governing equations of the current phase are:

a) The pressure at position O of rod-target interface P_o [15]:

For $u \geq U_{Fo}$:

$$P_o = R_t + \frac{1}{2}\rho_t u^2 = Y_P + \frac{1}{2}\rho_P (v-u)^2 \quad (1)a$$

where

$$R_t = 2\rho_t \delta(u)^2 + S - \rho_t u \delta(u) \quad (1)b$$

and

$$\delta(u) = U_{F0}.exp\left[-\left(\frac{u-U_{F0}}{nU_{F0}}\right)^2\right]. \quad (1)c$$

For $u < U_{Fo}$:

$$P_o = S + C\rho_t u^2 = Y_P + \frac{1}{2}\rho_P (v-u)^2 \quad (1)d$$

R_t is the target strength factor, u is the penetration velocity,ρ_t and ρ_p are the densities of rod and target materials, respectively,δ(u) is the particlevelocity at position B, S is the static target resistance, C is the constant of dynamic resistive pressure and is equal to 3/2 for incompressible materials, v is the velocity of rod rigid part, Y_P is the rodstrength factor, U_{Fo} is the critical penetration velocity and n is constant which is equal to 2.45.

The rod strength factor Y_P is equivalent to Hugoniot Elastic limit $(HEL)_P$of its material as reported in Ref. [18] whereas; the critical penetration velocity U_{Fo} is equivalent to $\sqrt{(HEL)_t/\rho_t}$. The subscripts P and t refer to rod and target, respectively.

The static target resistance is determined by [19]:

$$S = \frac{2Y_t}{3}\left[1 + \left(1 - \frac{E_{2t}}{E_{1t}}\right) ln\left(\frac{2E_{1t}}{3Y_t}\right)\right] + \frac{2}{27}\pi^2 E_{2t} \quad (2)$$

where Y_t,E_{1t} and $E_{2t}$are yield strength, elastic and plastic modulii of target material, respectively.

From Eqn. (1)a, the current penetration velocity can be calculated as a function of velocity of rod rigid part (v) when the target flow region exists. Equation (1)d determines the current penetration velocity as function of v when plastic and elastic regions are dominated in the target.

b) From the equation of motion of rod rigid part, the deceleration of its rigid mass during the penetration process is represented by:

$$\frac{dv}{dt} = -\frac{Y_p}{\rho_p . l}, \quad (3)$$

wherel is the current length of rod rigid mass.

c) The decreasing rate of length of rod rigid part is:

$$\frac{dl}{dt} = -(v-u). \quad (4)$$

d) The time rate of change of primary penetration depth of rodinto target is:

$$\frac{dZ_P}{dt} = u \quad (5)$$

where$Z_p$is the rod penetration depth in the primary penetration phase.

e) The current diameter of crater D_C which is represented by [20]:

$$\frac{D_C}{D_o} = \sqrt{\frac{Y_P + \rho_P(\phi+1)(v-u)^2}{S}} \tag{6}$$

where

$$\phi = \sqrt{1 - \frac{2\,Y_P}{\rho_P\,(v-u)^2}}\ . \tag{6a}$$

f) The velocity of rod rigid mass $V_C$is represented by:

$$V_C = U_{FO} + \sqrt{\frac{2(S + C\,\rho_t\,U_{FO}^2 - Y_P)}{\rho_P}}. \tag{7}$$

and

g) The interface defeat velocity $V_{ID}$is represented by:

$$V_{ID} = \sqrt{2(S - Y_P)/\rho_P}\,. \tag{8}$$

For $u \geq U_{FO}$, equations (3), (4), (5) and (6) in addition to Eqn. (1)arepresents a system of equationsthat solved numerically.The initial conditions for solving this system are:

$$at\ \ t = 0.0,\ v = v_i,\ u = u_i,\ l = l_o + \frac{2}{3}r_o,\ Z_p = 0.0\ \ and\ D = D_o$$

When $v < V_C$, the same system of equations is used after replacing equation (1)a by (1)d. This is meant that there is no flow region in the target; i.e. the plastic and elastic regions are only exist. This system is also used when the impact velocity $v_i < V_C$. The penetration process is continued until the velocity of rod rigid part v reaches a velocity named interface defeat velocity, V_{ID} (c.f. Eqn. (8)).

Based on the impact velocity of rod into target; the condition terminating the primary penetration phase is: (i) when the length of rod is totally consumed or (ii) when the penetration velocity u reaches zero.

2.2.2.After-flow penetration phase. The Tate's empirical equations [21] are employed to calculatethe depth of penetration which occurs in the after-flow phase. Thedepth of penetration Z_{a-f} is evaluated by:

$$Z_{a-f} = \frac{D_{cp}}{4}\left[\left(1 + \frac{3\rho_P u_i^2}{2R_{spt}}\right)^{1/3} - 1\right], \tag{9}$$

Where D_{Cp} is the diameter of the crater at the end of primary penetration phase, u_i is the penetration velocity corresponding to the initial impact velocity v_i, and R_{spt} is evaluated by the following equation:

$$R_{spt} = \frac{2Y_t}{3}\left[1 + ln\left(\frac{2E_{1t}}{3Y_t}\right)\right]. \tag{10}$$

The total depth of penetration of rod into target Z at the end of penetration process is the sum of penetration depth at the end of primary penetration phase Z_{pt} and that of the after-flow phase Z_{a-f}; i.e.

$$Z = Z_{pt} + Z_{a-f}.$$

The governing equations representing the penetration process due to the impact of high-speed long rods into semi-infinite metallic targets are converted into a computer program. The input data to the program are diameter of hemispherical-cylindrical rod and its length as well as its mechanical properties (density, yield strength, modulus of elasticity and Poisson's ratio), and impact velocity in addition to the mechanical properties of the target material (density, yield strength, moduliof elasticity and plasticity and Poisson's ratio).

The present model is capable of predicting time-histories of the velocity of rod rigid mass, the penetration velocity, the rod penetration depth into target, the length of rod rigid mass and the crater diameter in the target. Moreover, the model is also capable of predicting the total depth and total time of penetration process, respectively. Experimental measurements of Ref. [22]have been used to

validate the model predictions. In addition, samples of the model predictionswill be presented with relevant analyses and discussions.

3. Numerical simulation

In the following, Autodyn-2D hydrocode simulates the penetration process of long rods into semi-infinite metallic targets at different impact velocities using the data of tested rods and targets of Ref. [22]. The tested rods, with aspect ratios of 10, were made of tungsten alloy having different mechanical properties. In addition, the tested semi-infinite metallic targets were made of steel with different mechanical properties. For groups 1,the rod is designated by D17 whereas; the target is designated by St-52. For group 2,the rod is designated by D17.6whereas; the target is designated by HzBA. For each group, the rod strikes the target normally with wide range of impact velocities.

3.1. Material description

3.1.1. Rod material. For each group, the input data of the rod material to the hydrocode are listed in Table 1. The equation of state of each rod material was selected to be shock; the erosion model was selected to be incremental geometrical strain. Both the strength and failure models of the rod material were selected to be Johnson-Cook model [23].

3.1.2. Target material. For each group, the input data of the target material to the hydrocode are listed in Table 1.For each target material, linear equation of state and erosion model of incremental geometric strain was selected. Johnson-Cook model was used as strength and failure models, respectively.

The main dimensions of rod and target (x and y) for each interaction are converted into sub-grids with vertical and horizontal lines (grid lines) as shown in figure 2. The main procedures representing the interaction problem using Autodyn-2D hydrocode are reported in Ref. [23]. The numerical results of Aurodyn-2D hydrocode will be validated with the available experimental measurements of Ref. [22] and they are used to assess the predictions of the present analytical model.

3.2. Mesh sensitivity

It is well known that the density of mesh affects the simulation results. In general, simulation with fine meshes produces appropriate solution; but it takes a longer time than that needed with coarse meshes. Therefore, the mesh density was taken to be fine along the penetration depth into target while the coarse meshes were taken away of the penetration direction. The mesh sensitivity study for the penetration of a long rod into a semi-infinite metallic target was done for each group of rod-target interaction at three different impact velocities. It was predicted that the mesh size at the penetration zone is 0.25 x 0.25 mm for the rod and target, respectively. This size gave a close penetration depth to the corresponding measured value of Ref. [22] at each tested impact velocity.

Table 1. Input data of tungsten alloy rods and steel targets to the code [22].

Parameter	**Value**			
	Group 1		Group 2	
	Rod	Target	Rod	Target
Material designation	D17	St-52	D17.6	HzBA
Reference Density, (g/cm^3)	17	7.85	17.6	7.85
Reference Temperature, (K)	300			
Rod length, (mm)	60	--	58	--
Rod diameter, (mm)	6	--	5.8	--
Specific heat (C.V.), (J/ kg K)	134	477	134	477
Shear modulus, (kPa)	160×10^6	73×10^6	160×10^6	73×10^6

Yield stress, (kPa)	985	500	1360	849
Hugoniot Elastic Limit, HEL (MPa)	1665	---	2312	---
Melting temperature, (K)	1723	1573	1723	1573
Erosion strain,	1.0	1.25	1.0	1.25

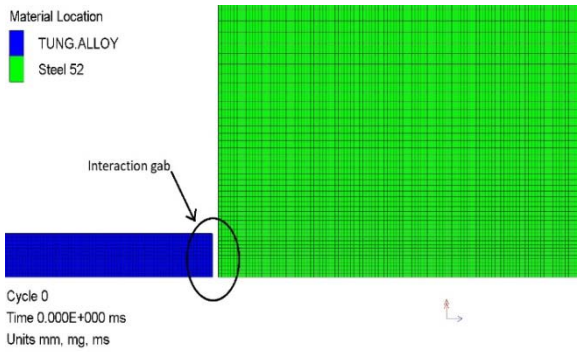

Figure 2. Representative D17 rod and St-52 target into Autodyn-2D hydrocode.

4. Results and discussions

In the following, the results of the analytical model are classified into: (i) validation and (ii) predictions. For each group of rod-target interaction, the validation is concerned with comparing the predicted penetration depths and crater radii obtained by the analytical model and Autodyn-2D hydrocode, respectively, at different impact velocities with the corresponding experimental measurements of Ref. [22]. In predictions, samples of the time-histories of the parameters associated with the penetration process and the corresponding simulation results of Autodyn-2D hydrocode are presented and discussed.

4.1. Validation

The predicted results of the analytical model and Autodyn-2D hydrocode are validated, respectively, with the corresponding experimental measurements of Anderson et al. [22]. They listed the measured penetration depths and surface crater diameters due to the impact of D17 tungsten alloy rod into St-52 steel semi-infinite target over a wide range of impact velocities. The input data of rod and target materials, respectively, to the model and Autodyn-2D hydrocode are listed in Table 1. The predicted change of penetration depths obtained by the model and hydrocode with impact velocity are depicted into figure 3a. The corresponding experimental measurements of Ref. [22] are also depicted in the same figure. Moreover, figure 3b plots the predicted change of surface crater diameters obtained analytically and numerically as well as the corresponding measurements of Ref. [22] with impact velocity.

Good agreement is generally obtained between the predictions of the analytical model and simulation

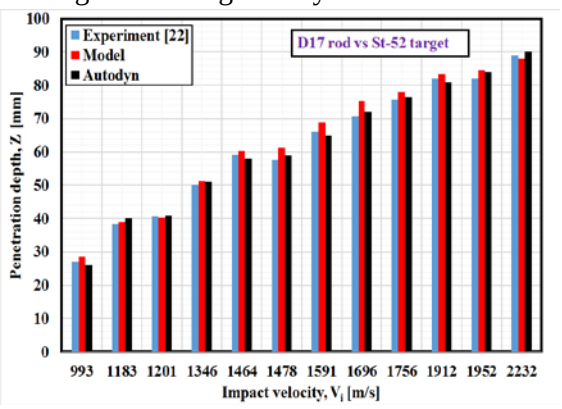

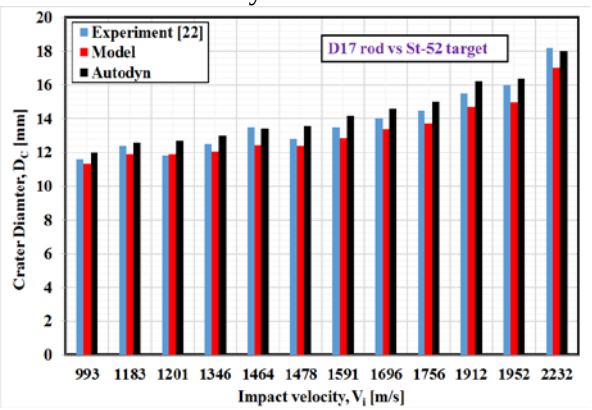

Figure 3a. Predicted change of penetration depth with rod impact velocity obtained by analytical model and Autodyn-2D hydrocode, respectively; measured depths of Ref. [22].

Figure 3b. Predicted change of crater diameter with rod impact velocity obtained by analytical model and Autodyn-2D hydrocode, respectively; measured diamters of Ref. [22].

results of Autodyn-2D hydrocode, respectively, and the corresponding experimental measurements of Ref. [22].The maximum absolute errors between the measured depth and the corresponding predicted one obtained by the model and Autodyn hydrocode, respectively, are found to be 8.2% at v_i = 1005 m/s and2.5% at v_i = 1632 m/s. In addition, the maximum absolute errors between the predicted surface diameters obtained analytically and numerically with the corresponding measurements are found to be 8.4% at v_i = 1982 m/s and 2.9% at v_i = 1909 m/s, respectively.

Another validation of the present model and Autodyn-2D hydrocode, respectively, is performed. Their predictive capabilities are tested using another measured data of Ref. [22] due to the impact of 17.6 tungsten alloy rods into HzBA steel targets at different impact velocities. The input data of rod and target materials to the model and hydrocode are listed in table 1. Figure 4a plots the predicted change of rod penetration depths obtained analytically, numerically and experimentally [22] with impact velocity. Similarly, figure 4b plots the predicted change of surface crater diameters with impact velocity.

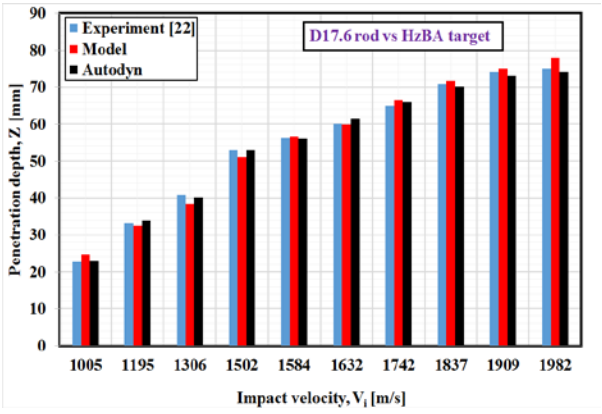

Figure 4a. Predicted change of rod penetration depth with impact velocity obtained by the analytical model and Autodyn-2D hydrocode, respectively; measured depths of Ref. [22].

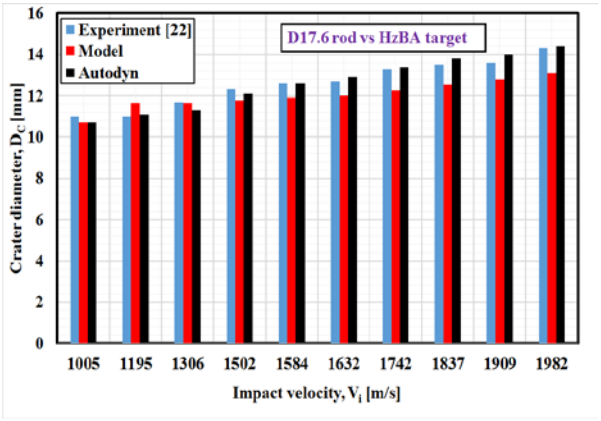

Figure 4b. Predicted change of crater diameter with rod impact velocity obtained by the analytical model and Autodyn-2D hydrocode, respectively; measured diamters of Ref. [22].

The obtained analytical and numerical results are consistent with the corresponding experimental measurements of Ref. [22]. The obtained results prove the predictive capabilities of the analytical model and Autodyn-2D hydrocode. The maximum absolute errors between the predicted penetration depths obtained analytically and numerically with the corresponding measurements are found to be 6.4% at v_i = 1696 m/s and 3.7% at v_i = 993 m/s, respectively. In addition, the maximum absolute errors between the predicted surface diameters obtained analytically and numerically with the corresponding measurements are found to be 6.38% at v_i = 1952 m/s and 7.63% at v_i = 1201 m/s, respectively.

4.2. Predictions

Figure 5a plots the predicted time-histories of the velocity of rod rigid part and the penetration velocity due to the impact of D17 rod into St-52 target at different velocities. At each impact velocity, it is seen from the figure that the velocity of rod rigid part, v, is slightly decreased at the beginning of penetration process however, the decreasing rate of this velocity increases gradually until the end of

the penetration process due to the increase of rod erosion. The rod front is subjected to erosion during the whole penetration process, the target flow region (FP) in front of eroded rod is replaced with plastic region when $v < V_C$. Similarly, the penetration velocity of the rod front, u, follows the same trend as the velocity of rod rigid part and the target penetration stops when u = 0.0; i.e. when the corresponding velocity v is equal to the velocity V_{ID} (=464 m/s). At the highest impact velocity, the penetration process is terminated due to the total consumption of the rod. It is also seen from this figure that the total time of penetration increases with the decrease of impact velocity. The predicted total penetration times are 80.2, 96 and 112 μs at v_i = 1952, 1346 and 993 m/s, respectively. The trends of the model predictions are similar to that presented in Refs. [10,13].

Figure 5b plots the time-histories of the velocity of rod rigid part due to the impact of D17 rod into St-52 target at different velocities predicted by the analytical model and Autodyn-2D hydrocode, respectively. At each impact velocity, it is seen from the figure that the predicted deceleration of the rod into target obtained by the model is consistent with the corresponding deceleration obtained by Autodyn hydrocode; except at the end of the penetration process where the deceleration of the rod obtained by Autodyn is slightly greater than that predicted by the model. This may be attributed to the difference in erosion rate of the rod length (v-u) and its influence on the predicted deceleration of rigid rod part. In addition, the difference on remaining lengths of rod rigid parth as a small influence on the total rod penetration depths into target. The predicted total penetration times obtained by the analytical model are 80.2, 96 and 112 μs and by Autodyn hydrocode are 84, 100 and 114 μs at v_i = 1952, 1346 and 993 m/s, respectively.

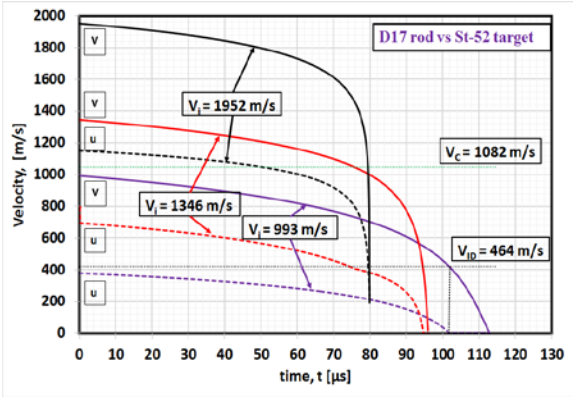

Figure 5a. Predicted time histories of velocity of rod rigid part and penetration velocity due to the impact of D17 rod into St-52 target at different velocities.

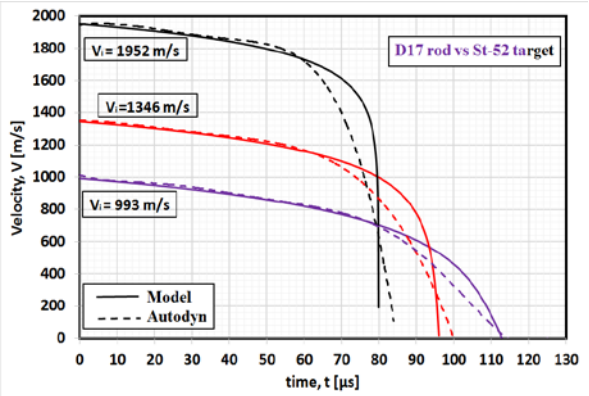

Figure 5b. Predicted time histories of velocity of rod rigid part and the corresponding predictions of Autodyn-2D due to the impact of D17 rod into St-52 target at different velocities.

Figure 6a plots the time histories of the velocity of rod rigid part, v, and the penetration velocity, u, due to the impact of D17.6 rod into HzBA target at different velocities. At each impact velocity, similar trends as that presented for the velocity, v, and the penetration velocity, u, in figure 5a are presented. It is also predicted that the rod is completely consumed at v_i = 1982 m/s. For the other two impact velocities, small rigid rod parts are remained at the end of penetration process. The predicted total penetration times obtained by the analytical model are 76.8, 91 and 107 μs at v_i = 1982, 1306 and 1005 m/s, respectively.

In addition, figure 6b depicts the time-histories of the velocity of D17.6 rod rigid part that predicted by the model and Autodyn hydrocode, respectively, at different velocities. Similar to that presented in figure 5b, good agreement is obtained between the velocity-time histories obtained by the model and Autodyn hydrocode except at the end of penetration process when v_i = 1982 m/s. The predicted total times of penetration predicted by the model are compared with that of Autodyn hydrocode and the maximum absolute error between them is found to be 5.49% at v_i = 1306 m/s.

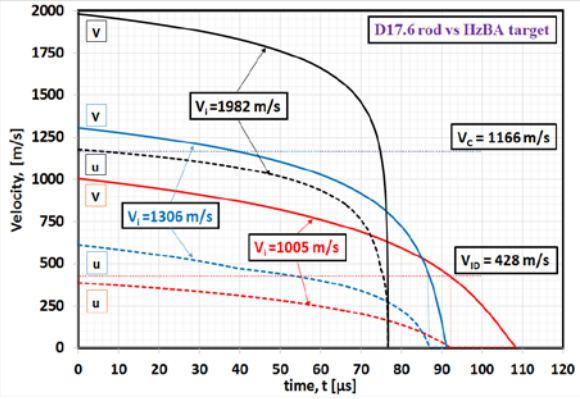

Figure 6a. Predicted time histories of velocity of rod rigid part and penetration velocity due to the impact of D17.6 rod into HzBA target at different velocities.

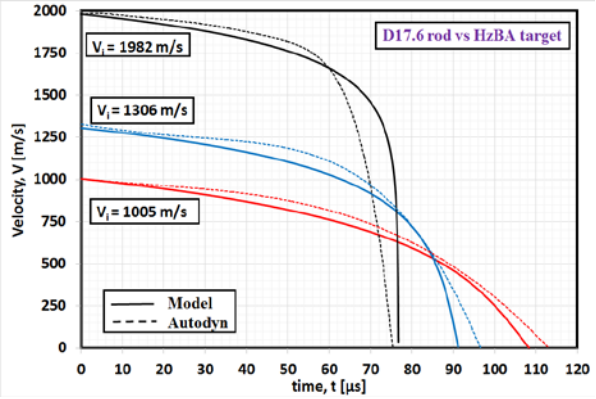

Figure 6b. Predicted time histories of velocity of rod rigid part and the corresponding predictions of Autodyn-2D due to the impact of D17.6 rod into HzBA target at different velocities.

Figure 7a plots the time-histories of the penetration depth due to the impact of D17 rod into St-52 target at different velocities. The corresponding predicted time-histories obtained by Autodyn hydrocode are depicted on the same figure. It is seen from the figure that the depth of penetration increases with the impact velocity; this is due to the increase of the penetration velocity with impact velocity. At each impact velocity, it is also seen from the figure that the predicted depth-time history of the analytical model is consistent with that obtained by Autodyn hydrocode. The maximum absolute errors between the model prediction and that of Autodyn hydrocode are 2.48%, 2.95% and 1.24% at v_i = 993, 1346 and 1952 m/s, respectively. Moreover, figure 7b plots the depth-time histories due to the impact of D17.6 into HzBA target at different velocities. Similar trends for the depth-time histories as that presented in figure 7a are plotted. In addition, the maximum absolute errors between the model prediction and that of Autodyn hydrocode are 5.7%, 3.9% and 0.39% at v_i = 1005, 1306 and 1982 m/s, respectively.

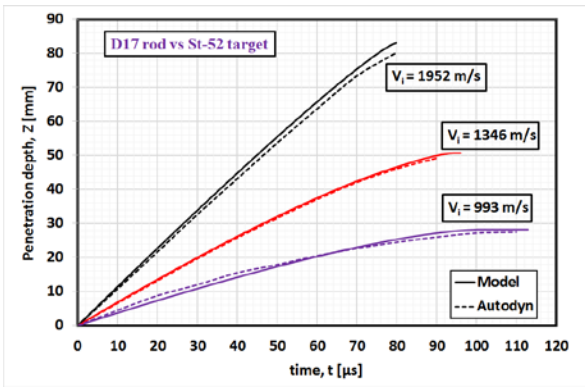

(a)

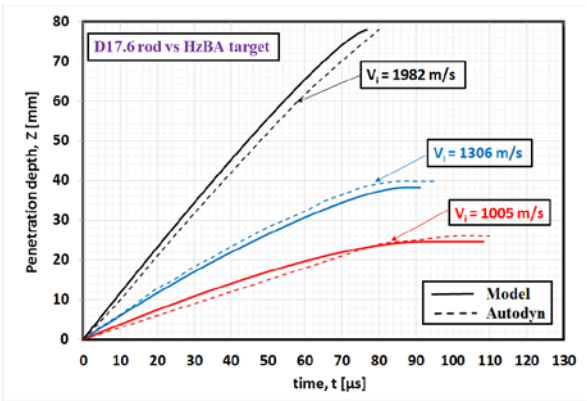

(b)

Figure 7. Predicted time histories of penetration depth and the corresponding predictions of Autodyn-2D due to the impact of: a) D17 rod into St-52 target and b) D17.6 rod into HzBA target at different velocities.

The present analytical model is used to predict the penetration depth during after-flow phase due to the impact of D17 rod into St-52 target over wide range of velocities. The obtained penetration depth represents 2.8% and 3.45% from the total penetration depth at impact velocities of 993 and 2232 m/s, respectively. This percent could be increased with impact velocity. Moreover, the depth of penetration of after flow phase due to the impact of D17.6 into HzBA target represents 2.18% and 2.95% from the

total depths at v_i = 1005 and 1982 m/s, respectively. The obtained results are similar to that predicted by Lan and Wen [15].

Figure 8a depicts the time-histories of rigid rod length due to the impact of D17 rod into St-52 target at different velocities. The corresponding time-histories obtained by Autodyn hydrocode are plotted on the same figure. At each impact velocity, it is seen from the figure that the length of rod rigid part decreases due to continuous erosion of its front during penetration. At the highest impact velocity, the rod is completely consumed during penetration whereas; tines of rigid rod lengths are remained at the end of penetration process for the other two impact velocities. This is attributed to the high erosion rate (v-u) at the highest impact velocity compared with the other two velocities which leads to the complete erosion of the rod length at the end of penetration process. It is also seen from the figure that the predicted rigid rod length-time history by the analytical model is consistent with that obtained by Autodyn hydrocode at each impact velocity. The predicted remaining rigid rod lengths at the end of penetration process of D17 rod into St-52 target obtained by the analytical model are 2.25, 0.45 and 0.0 mm whereas; the corresponding predictions by Autodyn hydrocode are 3.0, 1.0 and 0.0 at v_i = 993, 1346 and 1952 m/s, respectively.

Moreover, figure 8b plots the rod rigid length-time histories due to the impact of D17.6 into HzBA target at different velocities. Similar trends for the rod rigid length-time histories as that presented in figure 8a are presented. In addition, the predicted remaining lengths of the rod by the model are 4.5, 1.35 and 0.0 whereas; the corresponding predictions by Autodyn hydrocode are 4.5, 1.8, and 1.0 at v_i = 1005, 1306 and 1982 m/s, respectively.

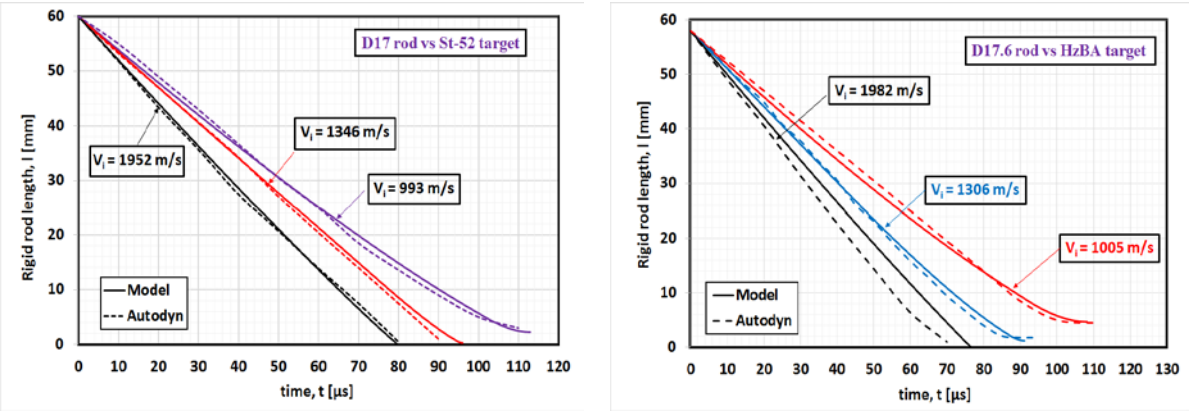

(a) (b)

Figure 8. Predicted time histories of rigid rod length and the corresponding predictions of Autodyn-2D due to the impact of: a) D17 rod into St-52 target and b) D17.6 rod into HzBA target at different velocities.

5. Conclusions

The main conclusions of the present work are:

- The analytical model of Lan and Wen [15] has been used herein to describe the penetration of semi-infinite metallic targets by long rods over a wide range of impact velocities. The target strength factor is not considered as a constant during penetration but; it is considered as a function of penetration velocity. The predictions of the model are compared with the available experimental measurements of Ref. [22], good agreement is generally obtained.
- The depth of penetration during the after flow phase is shallow at low impact velocity; and it has a considerable value when the impact velocity exceeds 2 km/s.
- Autodyn-2D hydrocode simulates the penetration of long rods into semi-infinite metallic targets using the rod and target data that fed into analytical model. The numerical results are compared with the available experimental measurements of Ref. [22] and the model predictions; good

agreement is generally obtained. In addition, the time-histories of penetration parameters that predicted by the analytical model and Autodyn-2D hydrocode are in good consistent.

- The obtained analytical results of the analytical model and numerical results of Autodyn-2D hydrocode reflect their predictive capabilities; each of them could be used as a quick tool for predicting the main parameters associated with the penetration of a long rod into a semi-infinite target over wide range of impact velocities.

References

[1] Alekseevskii VP1966Penetration of a rod into a target at high velocity*Combustion, Explosion and Shock Waves* **2** pp 63-6.
[2] Tate A1967 A theory for the deceleration of long rods after impact*J. Mech. Phys. Solids* **15** pp 387–99.
[3] Jones SE, Gills PP and FosterJ C1987On the penetration of semi-infinite targets by long rods*J. Mech. Phys. Solids* **35** pp 121-31.
[4] Wilson LL, Foster JC, Jones JC, Jr and Gillis PP1989Experimetal rod impact results*Int. J. Impact Engng.* **8**1 pp 5-25.
[5] He Yand Wen H M2013 Predicting the Penetration of Long Rods into Semi-Infinite Metallic Targets *Sci. CHINA* **56** pp 2814–20.
[6] Silsby G F1984Penetration of semi-infinite steel targets by tungsten rods at 1.3 to 4.5 km/s *Proc. of 8th Int. Symp. on Ballistics* (Orlando Florida **TB**/31-5.)
[7] Cullis I G and Lynch N J1994Hydrocode and experimental analysis of scale size jacketed ke projectiles*Proc.14th Int. Symp. on Ballistics* (Quebec, Canada **TB-7** 271-80).
[8] Anderson Jr. CE2017Analytical models for penetration mechanics: A review", *Int. J. Impact Engng*. **108** pp 3-26.
[9] Anderson Jr. CE, Littlefield DL and Walker JD1993Long rod penetration, target resistance and hypervelocity impact*Int. J. Impact Engng.***14** pp 1-14.
[10] Walker JD and Anderson Jr CE1995A time dependent model for long rod penetration*Int. J. Impact Engng.***16** pp 19-48.
[11] Chocron S, Anderson Jr CE and Walker JD1998Long rod penetration: Cylindrical vs spherical cavity expansion for the extent of plastic flow", *Proc. 17th Symp. on Ballistics*, South African Ballistics Organization pp319-26.
[12] Jiao WJ and Chen XW2018Approximate solutions for Alekseevskii-Tate model of long-rod penetration *Acta Mech. Sin.***34 pp** 334-48.
[13] Anderson Jr. CE and Walker JD1991An examination of long rod penetration*Int. J. Impact Engng.* **11** pp 481-501.
[14] Walter W, Williams Cand Normandia M2006An explicit soluion of Alekseevskii-Tate penetration equations*Int. J. Impact Engng*. **33** pp 837-46.
[15] Lan Band Wen HM2010 Alekseevskii-Tate revisited: An extension to the modified hydrodynamic theory of long rod penetration *Sci. CHINA* **53** pp 1364–373.
[16] Lan Band Wen H M2008Numerical simulation and analysis of the penetration of tungesten alloy long rods into semi-infinite steel targets *Chinease J. High Pressure Physics***22** 245-52.
[17] Forrestal M J and Luk V K 1988Dynamic cavity-expansion in a compressible elastic-plastic solid *J. Appl. Mech.***55** pp 275-79.
[18] Lan Band Wen H M2009Numerical simulation of the penetratin of a spherical-nosed 4340 steel long rod into semi-infinite 6061-t6511 aluminium targets", *J. Eng. Mech*. **26** 183-190.
[19] Lu Z C and Wen H M2017On the penetration of high strength steel rods into semi-infinite aluminium alloy targets *Int. J. Impact Eng*. **111** pp 1–10.
[20] Wen H M, He Yand Lan B2010Analytical model for cratering of semi-infiniye metal targets by long rod penetration *Sci. ChinaTech Sci.***53** pp 3189-196.
[21] Tate A 1986A long rod penetration models-part ii. extensions to the hydrodynamic theory of penetration *Int. J. Mech Sci.***28** pp 599-612.

[22] Anderson Jr CE, Morris BL and Littlefield D1992A penetration mechanics database *Report No. 3593/C01* San Antonio, Texas, U.S.A. Southwest Research Institute.
[23] AUTODYN 2016Interactive non-linear dynamics analysis software *Century Dynamics Inc.*